Inorganica Chimica Acta 425 (2015) 67–75

Contents lists available at ScienceDirect

Inorganica Chimica Acta

journal homepage: www.elsevier.com/locate/ica

Palladium complexes of 2-formylpyridine thiosemicarbazone and two related ligands: Synthesis, structure and, spectral and catalytic properties

Piyali Paul [a], Ray J. Butcher [b], Samaresh Bhattacharya [a,*]

[a] Department of Chemistry, Inorganic Chemistry Section, Jadavpur University, Kolkata 700 032, India
[b] Department of Chemistry, Howard University, Washington, DC 20059, USA

ARTICLE INFO

Article history:
Received 9 June 2014
Received in revised form 8 October 2014
Accepted 9 October 2014
Available online 22 October 2014

Keywords:
2-Formylpyridine thiosemicarbazone
Palladium complexes
Syntheses
Structures
C–C and C–N coupling reactions

ABSTRACT

Thiosemicarbazones of 2-formylpyridine, 2-aceylpyridine and 2-benzoylpyridine, abbreviated in general as **HL-R** (where H depicts the acidic hydrogen and R the fragment (R = H, Me and Ph) linked to the imine-carbon) react with $[Pd(PPh_3)_2Cl_2]$ in refluxing ethanol in the presence of triethylamine to afford complexes of the type $[Pd(L\text{-}R)(PPh_3)]Cl$ (**1**, R = H; **2**, R = Me, **3**, R = Ph). Structures of the complexes **1** and **3** have been determined by X-ray crystallography, and the structure of complex **2** has been optimized by DFT. In all three the thiosemicarbazone ligand binds to the metal center as a monoanionic tridentate NNS-donor forming two adjacent five-membered chelate rings, the triphenylphosphine occupies the fourth coordination site on palladium. Complexes **1**–**3** display intense absorptions in the visible and ultraviolet regions, which have been analyzed by TDDFT calculations. All the complexes are found to efficiently catalyze Suzuki, Heck and Sonogashira type C–C cross-coupling, and C–N coupling reactions of aryl halides with primary and secondary amines. All the catalytic reactions are found to proceed under ligand-free condition.

1. Introduction

Thiosemicarbazone complexes of the transition metals have received considerable attention, largely because of their bioinorganic relevance [1]. However, we have been exploring the chemistry of transition metal complexes of the thiosemicarbazones, primarily because of the variable binding mode displayed by these ligands in their complexes, and the present work has emerged out of this exploration [2]. In a recent study we have observed that benzaldehyde thiosemicarbazone (**HL**), and four similar ligands, react with $[Pd(PPh_3)_2Cl_2]$ to yield a group of mixed-ligand complexes of type $[Pd(PPh_3)(L)Cl]$ (Scheme 1), in which the thiosemicarbazones display a NS-mode of coordination [2a,b]. In view of the structure of the uncoordinated thiosemicarbazone, which is similar to that shown for **HL** [2b], this NS-mode of coordination is a bit uncommon as it involves a change in geometry around the pre-existing C=N bond. In order to examine whether substitution of the phenyl ring in **HL** by a pyridyl ring, with the pyridine-nitrogen at the *ortho* position with respect to the imine group, can prevent this change in geometry via coordination of the pyridine-nitrogen to the metal center, we have selected the thiosemicarbazone of 2-formylpyridine, and two related ligands, *viz.* thiosemicarbazones of 2-aceylpyridine and 2-benzoylpyridine, for the present study. The chosen thiosemicarbazones are abbreviated in general as **HL-R**, where H depicts the acidic hydrogen and R the fragment (R = H, Me and Ph) linked to the imine-carbon. The main aim of the present work has been to study the interaction of the selected thiosemicarbazones (**HL-R**) with $[Pd(PPh_3)_2Cl_2]$ and see whether they bind to palladium in an NNS-mode (**I**) without any rotation around the pre-existing imine bond. The other, and equally important, objective has been to

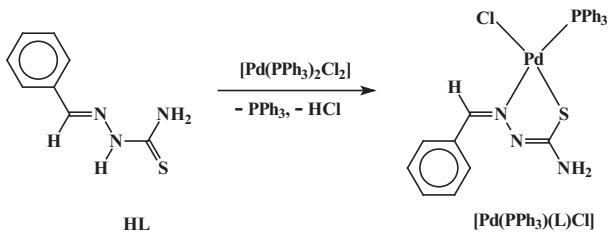

Scheme 1.

* Corresponding author.
E-mail address: samaresh_b@hotmail.com (S. Bhattacharya).

http://dx.doi.org/10.1016/j.ica.2014.10.010
0020-1693/

explore catalytic activity of the resulting complexes towards coupling reactions of various types. It may be worth mentioning here

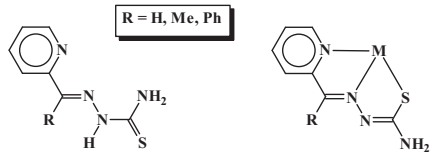

that palladium complexes are extensively utilized as catalyst for the synthesis of industrially useful organic molecules, particularly via C–C and C–N coupling reactions [3,4]. Reactions of the chosen thiosemicarbazones with $[Pd(PPh_3)_2Cl_2]$ have been found to afford a group of mixed-ligand complexes, and the chemistry of these complexes is reported in this paper, with particular reference to their formation, structure and, catalytic efficiency towards C–C and C–N coupling reactions.

2. Experimental

2.1. Materials

Palladium chloride was obtained from Arora Matthey, Kolkata, India. The $[Pd(PPh_3)_2Cl_2]$ complex was prepared by following a reported procedure [5]. 2-Formylpyridine, 2-acetylpyridine and 2-benzoylpyridine were obtained from Merck (India), Spectrochem (India) and Sigma–Aldrich, respectively. The thiosemicarbazone ligands (**HL-R**; R = H, Me and Ph) were prepared by reacting equimolar amounts of thiosemicarbazide and the respective pyridine-derivative in warm ethanol [6]. All other chemicals and solvents were reagent grade commercial materials and were used as received.

2.2. Preparation of the complexes

The [Pd(L-R)(PPh_3)]Cl complexes (**1**, R = H; **2**, R = Me; **3**, R = Ph) were prepared by following a general procedure. Specific details are given below for a particular complex.

2.2.1. Complex *1*

2-Formylpyridine thiosemicarbazone (26 mg, 0.14 mmol) was dissolved in warm ethanol (30 mL) and triethylamine (14 mg, 0.14 mmol) was added to it, followed by $[Pd(PPh_3)_2Cl_2]$ (100 mg, 0.14 mmol). The mixture was then refluxed for 5 h to yield a yellowish–brown solution. The solvent was evaporated and the solid mass, thus obtained, was subjected to purification by thin layer chromatography on a silica plate. With 1:3 acetonitrile-benzene as the eluant, an orangish–yellow band separated, which was extracted with acetonitrile. Evaporation of the acetonitrile extract gave complex **1** as an orangish–yellow crystalline solid. Yield: 68%. *Anal.* Calc. for $C_{25}H_{22}N_4PSClPd$: C, 51.47; H, 3.77; N, 9.61. Found: C, 51.53; H, 3.72; N, 9.65%. Mass spectral data (ESI, positive mode, CH_3CN): *m/z* 547 for $[1\text{-Cl}]^+$. Λ_M: 145 $^{-1}$ cm^2 M^{-1}. ^{1}H NMR (300 MHz, $CDCl_3$)[1]: 5.73 (s, NH_2), 7.19 (t, 1H, *J* = 9.0), 7.38 (s, 1H), 7.58–7.72 (PPh_3), 7.87 (d, 1H, *J* = 8.0), 8.06 (t, 1H, *J* = 8.5), 8.16 (d, 1H, *J* = 9.0). ^{31}P NMR (300 MHz, $CDCl_3$): 43.04 ppm. IR (cm^{-1}): 1646, 1602, 1562, 1480, 1458, 1434, 1375, 1318, 1255, 1179, 1098, 1020, 997, 752, 722, 697, 532, 508.

[1] Chemical shifts are given in ppm and multiplicity of the signals along with the associated coupling constants (*J* in Hz) are given in parentheses. Overlapping signals are marked with an asterisk.

2.2.2. Complex *2*

Yield: 62%. *Anal.* Calc. for $C_{26}H_{24}N_4PSClPd$: C, 52.27; H, 4.02; N, 9.38. Found: C, 52.23; H, 4.07; N, 9.36%. Mass spectral data (ESI, positive mode, CH_3CN): *m/z* 561 for $[2\text{-Cl}]^+$. Λ_M: 148 $^{-1}$ cm^2 M^{-1}. ^{1}H NMR (300 MHz, DMSO-d_6): 2.42 (s, CH_3), 5.69 (s, NH_2), 7.16 (t, 1H, *J* = 9.0), 7.59–7.68 (PPh_3), 7.80 (d, 1H, *J* = 8.0), 7.94 (t, 1H, *J* = 8.5), 8.10 (d, 1H, *J* = 9.0). ^{31}P NMR (300 MHz, DMSO-d_6): 43.03 ppm. IR (cm^{-1}): 1639, 1599, 1563, 1480, 1456, 1432, 1380, 1315, 1257, 1146, 1098, 1020, 998, 747, 721, 694, 531, 506.

2.2.3. Complex *3*

Yield: 71%. *Anal.* Calc. for $C_{31}H_{26}N_4PSClPd$: C, 56.46; H, 3.95; N, 8.50. Found: C, 56.51; H, 3.97; N, 8.46%. Mass spectral data (ESI, positive mode, CH_3CN): *m/z* 623 for $[3\text{-Cl}]^+$. Λ_M: 144 $^{-1}$ cm^2 M^{-1}. ^{1}H NMR (300 MHz, $CDCl_3$): 5.29 (s, NH_2), 7.07 (d, 1H, *J* = 9.0), 7.37–7.69 (PPh_3 + 2H*), 7.78 (t, 1H, *J* = 8.5), 7.93 (t, 1H, *J* = 8.2), 8.07 (t, 1H, *J* = 9.0), 8.73 (d, 2H, *J* = 9.0), 8.87 (d, 1H, *J* = 9.0). ^{31}P NMR (300 MHz, $CDCl_3$): 43.10 ppm. IR (cm^{-1}): 1616, 1596, 1545, 1482, 1454, 1437, 1384, 1320, 1263, 1181, 1097, 1027, 998, 745, 722, 695, 533, 510.

2.3. Physical measurements

Microanalyses (C, H and N) were performed using a Heraeus Carlo Erba 1108 elemental analyzer. Mass spectra were recorded with a Micromass LCT electrospray (Qtof Micro YA263) mass spectrometer. NMR spectra were recorded in $CDCl_3$ or DMSO-d_6 solution on a Bruker Avance DPX 300 NMR spectrometer. IR spectra were obtained on a Perkin Elmer Spectrum Two IR spectrometer with samples prepared as KBr pellets. Solution electrical conductivities were measured in acetonitrile solution using a Philips PR 8499 bridge with a solute concentration of 10^{-3} M. Electronic spectra were recorded on a JASCO V-570 spectrophotometer. Geometry optimization by density functional theory (DFT) method and electronic spectral analysis by TDDFT calculation were performed using the GAUSSIAN 03 (B3LYP/SDD-6–31G) package [7]. GC–MS analyses were performed using a Perkin Elmer CLARUS 680 instrument.

2.4. X-ray crystallography

Single crystals of complex **1** were obtained by slow evaporation of solvents from a solution of the complex in 1:1 methanol–acetonitrile. Single crystals of complex **3** were obtained by slow evaporation of solvent from a solution of the complex in acetonitrile. Selected crystal data and data collection parameters are given in Table 1. Data were collected on a Bruker SMART CCD diffractometer using graphite monochromated Mo Kα radiation (λ = 0.71073 Å). X-ray data reduction, structure solution and refinement were done using SHELXS-97 and SHELXL-97 programs [8]. The structures were solved by the direct methods. In the structure of complex **3**, there was severely disordered solvent present on crystallographic symmetry elements which could not be modeled. This was removed using the SQUEEZE routine from PLATON.

2.5. Application as catalysts

2.5.1. General procedure for the Suzuki coupling reactions

In a typical run, an oven-dried 10 mL round bottom flask was charged with a known mole percent of catalyst, Na_2CO_3 (1.7 mmol), phenylboronic acid (1.2 mmol) and aryl halide (1 mmol) with the appropriate solvents (4 mL). The flask was placed in a preheated oil bath at required temp. After the specified time the flask was removed from the oil bath and water (20 mL) added, followed by extraction with ether (4 × 10 mL). The combined organic layers were washed with water (3 × 10 mL), dried over anhydrous Na_2SO_4, and filtered. Solvent was removed under

Table 1
Crystallographic data for the complex **1** and complex **3**.

Complex	**1**·H_2O	**3**·3.75H_2O
Empirical formula	$C_{25}H_{24}N_4OPSClPd$	$C_{124}H_{134}N_{16}O_{15}P_4S_4Cl_4Pd_4$
Formula weight	601.36	2907.98
Crystal system	triclinic	monoclinic
Space group	$P\bar{1}$	$C2/c$
a (Å)	9.1746(2)	32.977(3)
b (Å)	9.4020(2)	15.1566(13)
c (Å)	15.5484(3)	31.115(4)
α (°)	107.030(1)	90
β (°)	95.493(1)	117.871(2)
γ (°)	95.559(1)	90
V (Å^3)	1265.46(5)	13748(2)
Z	2	4
D_{calc} (g cm^{-3})	1.578	1.405
λ (Å)	0.71073	0.71073
F(000)	608	5944
Crystal size (mm)	0.37 × 0.24 × 0.15	0.35 × 0.25 × 0.12
T (K)	298	173
μ (mm^{-1})	1.010	0.763
R_1[a]	0.0224	0.0745
wR_2[b]	0.0582	0.1537
Goodness-of-fit (GOF) on F^2[c]	1.062	0.956

[a] $R_1 = ||F_o| - |F_c||/|F_o|$.
[b] $wR_2 = [[w(F_o^2 - F_c^2)^2]/[w(F_o^2)^2]]^{1/2}$.
[c] Goodness-of-fit (GOF) = $[[w(F_o^2 - F_c^2)^2]/(M - N)]^{1/2}$, where M is the number of reflections and N is the number of parameters refined.

vacuum. The residue was dissolved in hexane and analyzed by GC–MS using Elite-5 columns, which are fused silica capillary columns coated with 5% diphenyl and 95% dimethyl polysiloxane.

2.5.2. General procedure for the Heck coupling reactions

In a typical run, an oven-dried 10 mL round bottom flask was charged with a known mole percent of catalyst, Cs_2CO_3 (1.7 mmol), *n*-butyl acrylate (1.2 mmol) and aryl halide (1 mmol) with polyethylene glycol (4 mL). The flask was placed in a preheated oil bath at 150 °C. After the specified time the flask was removed from the oil bath and water (20 mL) added, followed by extraction with ether (4 × 10 mL). The combined organic layers were washed with water (3 × 10 mL), dried over anhydrous Na_2SO_4, and filtered. Solvent was removed under vacuum. The residue was dissolved in hexane and analyzed by GC–MS using Elite-5 columns, which are fused silica capillary columns coated with 5% diphenyl and 95% dimethyl polysiloxane.

2.5.3. General procedure for Sonogashira coupling reactions

To slurry of aryl halide (1 mmol), cuprous iodide (10 mol%) and palladium catalyst (a known mol%) in an appropriate solvent (4 mL), phenylacetylene (1.2 mmol) and NaOH (1.7 mmol) was added and heated at required temp. After completion of the reaction (monitored by TLC), the flask was removed from the oil bath and water (20 mL) added, followed by extraction with ether (4 × 10 mL). The combined organic layers were washed with water (3 × 10 mL), dried over anhydrous Na_2SO_4, and filtered. Solvent was removed under vacuum. The residue was dissolved in hexane and analyzed by GC–MS using Elite-5 columns, which are fused silica capillary columns coated with 5% diphenyl and 95% dimethyl polysiloxane.

2.5.4. General procedure for C–N coupling reactions

In a typical run, an oven-dried 10 mL round bottom flask was charged with a known mole percent of catalyst, NaO^t–Bu (1.3 mmol), aryl amine (1.2 mmol) and aryl halide (1 mmol) with the appropriate solvent(s) (4 mL). The flask was placed in a preheated oil bath at required temp. After the specified time the flask was removed from the oil bath, water (20 mL) was added, and extraction with ether (4 × 10 mL) was done. The combined organic layers were washed with water (3 10 mL), dried over anhydrous Na_2SO_4, and filtered. Solvent was removed under vacuum. The residue was dissolved in hexane and analyzed by GC–MS using Elite-5 columns, which are fused silica capillary columns coated with 5% diphenyl and 95% dimethyl polysiloxane.

3. Results and discussion

3.1. Synthesis and characterization

The reaction between 2-formylpyridine thiosemicarbazone (HL-H) and $[Pd(PPh_3)_2Cl_2]$ proceeded smoothly in refluxing ethanol in the presence of triethylamine to afford an orangish-yellow complex **1** in a decent yield. Preliminary characterization (microanalysis, mass, IR, NMR, etc.) on complex **1** indicated the presence of a thiosemicarbazone and a triphenylphosphine in the coordination sphere. In order to unambiguously characterize this complex, and particularly to ascertain coordination mode of the thiosemicarbazone ligand in it, its structure was determined by X-ray crystallography. The structure (Fig. 1) shows that 2-formylpyridine thiosemicarbazone is coordinated to palladium, via dissociation of the acidic proton, as a monoanionic tridentate NNS-donor forming two adjacent five-membered chelate rings (I, R = H). A triphenylphosphine is also coordinated to the metal center. To balance the uni-positive charge of this tetra-coordinated palladium complex, a chloride ion exists outside the coordination sphere, which was also clearly found in the crystal structure. The structure determination also reveals that coordination by the pyridine-nitrogen has been effective, as anticipated, in preventing the rotation around the pre-existing imine bond, observed with benzaldehyde thiosemicarbazone [2a,b]. It is relevant to mention here that such NNS-mode of binding by this thiosemicarbazone ligands has precedence in the literature [9]. It may also be mentioned here that a palladium complex containing a dianionic NNS-coordinated thiosemicarbazone and PPh_3 is also reported in the literature [10]. The N_2SP coordination sphere around palladium is distorted considerably from ideal square planar geometry, as manifested in the bond parameters around the metal center (Table 2). The Pd–N, Pd–S and Pd–P distances are found to be normal, as observed in structurally characterized complexes of palladium containing these bonds [2a,b,9a].

To check the generality of the observed NNS-mode of coordination displayed by 2-formylpyridine thiosemicarbazone, reaction of $[Pd(PPh_3)_2Cl_2]$ was also carried out with the other two selected ligands, *viz.* 2-aceylpyridine thiosemicarbazone (**HL-Me**) and 2-benzoylpyridine thiosemicarbazone (**HL-Ph**), under similar experimental conditions as before, which afforded orangish-yellow com-

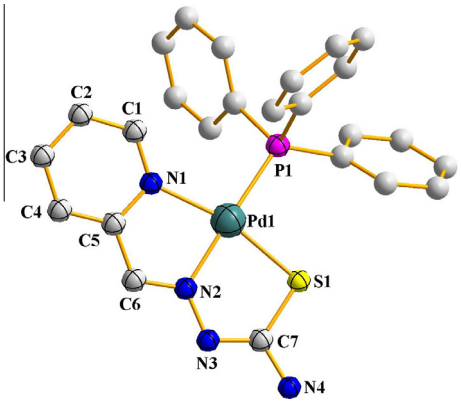

Fig. 1. View of the crystal structure of complex **1**. The chloride ion outside the coordination sphere is not shown.

Table 2
Selected bond lengths (Å) and bond angels (°) for the complexes **1** and **3**.

Complex **1**			
Bond lengths (Å)			
Pd(1)–N(1)	2.1035(16)	C(6)–N(2)	1.287(3)
Pd(1)–N(2)	2.0176(17)	N(2)–N(3)	1.357(3)
Pd(1)–P(1)	2.2780(5)	N(3)–C(7)	1.320(3)
Pd(1)–S(1)	2.2432(6)	C(7)–N(4)	1.322(3)
		C(7)–S(1)	1.773(2)
Bond angles (°)			
P(1)–Pd(1)–N(2)	177.59(5)	N(1)–Pd(1)–N(2)	80.49(6)
S(1)–Pd(1)–N(1)	163.51(5)	S(1)–Pd(1)–N(2)	83.20(5)
Complex **3**			
Bond lengths (Å)			
Pd(1)–N(1A)	2.079(4)	C(6A)–N(2A)	1.321(6)
Pd(1)–N(2A)	2.008(4)	N(2A)–N(3A)	1.363(6)
Pd(1)–P(1A)	2.2538(16)	N(3A)–C(13A)	1.319(7)
Pd(1)–S(1A)	2.2370(17)	C(13A)–N(4A)	1.336(7)
		C(13A)–S(1A)	1.764(6)
Bond angles (°)			
P(1A)–Pd(1)–N(2A)	176.48(12)	N(1A)–Pd(1)–N(2A)	80.25(18)
S(1A)–Pd(1)–N(1A)	164.64(14)	S(1A)–Pd(1)–N(2A)	84.50(13)

plexes **2** and **3**, respectively, in good yield. Preliminary characterizations on these complexes indicated that they also have composition similar to that of complex **1**. Structural characterization of complex **2** by X-ray crystallography was not possible, as single crystals of this complex could not be grown. However, its structure was geometrically optimized through DFT calculations [7]. The optimized structure of the complex cation is shown in Fig. S1 (Supplementary material) and some computed bond parameters are presented in Table S1 (Supplementary material). The optimized structure of complex **2** is found to compare well with the crystal structure of complex **1**. Structure of complex **3**, however, could be determined by X-ray crystallography, and the structure (Fig. 2) shows the same NNS-mode of binding (**I**, R = Ph) by the thiosemicarbazone ligand. The metrical parameters (Table 2) of this structure are also comparable to those observed for complex **1**. From the structural data it is evident that the pyridine-nitrogen in 2-formylpyridine thiosemicarbazone, and the other two related ligands, has been very effective in enabling these ligands to bind to palladium in the NNS-mode (**I**) and thus preventing the change in geometry around the pre-existing imine bond during their complexation.

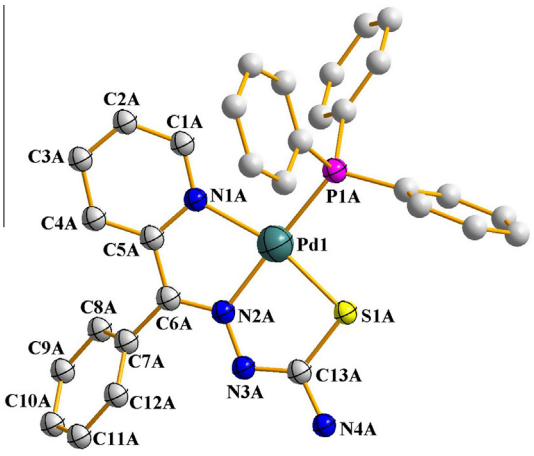

Fig. 2. View of the crystal structure of complex **3**. The chloride ion outside the coordination sphere is not shown.

3.2. Spectral studies

^{1}H NMR spectra of complexes **1**–**3** show broad signals within 7.37–7.72 ppm for the coordinated PPh_3 ligands, and a distinct signal at around 5.6 ppm for the NH_2 fragment. In complex **1**, a signal for the azomethine proton in the coordinated thiosemicarbazone appears at 7.38 ppm. In complex **2**, signal for the methyl group is observed at 2.42 ppm. In all the three complexes most of the aromatic proton signals are clearly observed in the expected region, while a few could not be detected due to their overlap with other signals in the same region. ^{31}P NMR spectra of complexes **1**–**3** show a single resonance within 43.03–43.10 ppm due to the coordinated PPh_3 ligand.

Infrared spectra of complexes **1**–**3** show many bands of different intensities in the 400–4000 cm^{-1} region. No attempt has been made to assign each individual band to a specific vibration. However, three strong bands have been observed near 532, 695, 748 and 1098 cm^{-1} in all the three complexes indicating the presence of coordinated PPh_3 ligands. Besides, comparison with the spectrum of $[Pd(PPh_3)_2Cl_2]$ shows the presence of several new bands (*e.g.* near 1646–1616, 1430, 1316 and 1179–1146 cm^{-1}) in the spectrum of complexes **1**–**3**, which are attributable to the coordinated thiosemicarbazone ligand.

Complexes **1** and **3** are found to be readily soluble in polar organic solvents like methanol, ethanol, acetonitrile, dichloromethane, chloroform, etc., producing intense yellow solutions. Complex **2**, however, is insoluble in dichloromethane and chloroform, but is soluble in the other polar organic solvents. Conductance measurement in acetonitrile solution shows that these complexes behave as 1:1 electrolytes as expected (see Section 2). Electronic spectra of the complexes were recorded in acetonitrile solutions. Spectral data are presented in Table 3. Each complex showed intense absorptions in the visible and ultraviolet regions. To have an insight into the nature of these absorptions, TDDFT calculations were performed on all three palladium complexes using the Gaussian 03 package [7]. Phenyl rings of the triphenylphosphines in complexes **1**–**3** were replaced by hydrogens for simplifying the calculation. The results of the TDDFT calculations for complex **1** are presented in Table 4, and those for complexes **2** and **3** are deposited in Table S2 and S3 (Supplementary material) respectively. Compositions of few frontier orbitals of complexes **1**–**3** are given in Table 5. Contour plots of some selected molecular orbitals for complex **1** are shown in Fig. 3 and those of all the orbitals, which are involved with the observed electronic spectral transitions, for all the three complexes are deposited as Figs. S2–S4 (Supplementary material). The results obtained are found to be qualitatively similar for all three complexes, and hence only the case of complex **1** is discussed here. The lowest energy absorption at 457 nm is attributable to a combination of HOMO → LUMO and HOMO-1 → LUMO transitions, and based on the nature of the participating orbitals (Table 5; Fig. 3) the electronic excitation is assignable to a mixture of MLCT, LMCT and LLCT transitions, involving primarily the thiosemicarbazone ligand, with much less contribution from the metal center. The next absorption at 416 nm is found to be due to a mixture of MLCT, LMCT, LLCT and ILCT transitions, again with thiosemicarbazone ligand as the major

Table 3
Electronic spectral data.[a]

Complex	λ_{max} (nm) (ε M^{-1} cm^{-1})
Complex **1**	457[b] (2300), 416 (2600), 355[b] (9500), 336 (9800), 295 (15000)
Complex **2**	455[b] (2100), 415 (2400), 353[b] (7300), 335 (8500), 297 (14200)
Complex **3**	460[b] (2000), 416 (2300), 358[b] (7100), 339 (7500), 299 (12000)

[a] In acetonitrile solution.
[b] Shoulder.

Table 4
Main calculated transitions for complex **1**[a] with composition in terms of molecular orbital contribution of the transition, excitation energies, and oscillator strength in acetonitrile.

Excited state	Composition	CI	*E* (eV)	Oscillator strength (*f*)	λ_{theo} (nm)	Assignments	λ_{exp} (nm)
1	H − 1 → L	−0.17848	2.7141	0.0417	456.81	MLCT/LMCT/LLCT	457
	H → L	0.65730				MLCT/LMCT/LLCT	
2	H − 1 → L + 1	−0.17959	2.8859	0.0021	429.62	MLCT/LMCT/LLCT/ILCT	416
	H → L + 1	0.64458				MLCT/LMCT/LLCT/ILCT	
3	H − 3 → L + 1	0.16285	3.4387	0.0124	360.56	MLCT/LMCT/LLCT/ILCT	355
	H − 4 → L + 1	0.27799				MLCT/LMCT/LLCT	
	H − 4 → L + 1	0.56789				MLCT/LMCT/LLCT/ILCT	
	H − 1 → L + 1	0.11252				MLCT/LMCT/LLCT/ILCT	
4	H − 4 → L	0.11187	3.6557	0.2276	339.15	MLCT/LMCT/LLCT/ILCT	336
	H − 4 → L + 1	0.11087				MLCT/LMCT/LLCT/ILCT	
	H − 1 → L	0.46419				MLCT/LMCT/LLCT	
	H − 1 → L + 1	0.40906				MLCT/LMCT/LLCT/ILCT	
	H → L + 1	0.12491				MLCT/LMCT/LLCT/ILCT	
	H → L + 2	−0.11608				MLCT/LMCT/LLCT	
5	H − 10 → L + 1	−0.13638	4.3077	0.0311	387.82	MLCT/LMCT/LLCT/ILCT	295
	H − 9 → L + 1	−0.19888				MLCT/LMCT/LLCT/ILCT	
	H − 5 → L + 1	−0.19363				MLCT/LMCT/LLCT/ILCT	
	H − 13 → L + 1	0.54077				MLCT/LMCT/LLCT/ILCT	
	H − 1 → L + 1	−0.13805				MLCT/LMCT/LLCT/ILCT	
	H → L + 2	0.19573				MLCT/LMCT/LLCT	

[a] PPh_3 was replaced by PH_3 in the calculation.

Table 5
Compositions of selected molecular orbitals of the complexes.[a]

Complex	Fragments	% Contribution of fragments to								
		H − 5	H − 4	H − 3	H − 2	H − 1	HOMO (H)	LUMO (L)	L + 1	L + 2
Complex **1**	Pd	10.1	23.6	25.6	43.1	19.9	18.5	8.7	26.4	7.3
	L–H	73.4	70.3	60.5	56.9	83.1	81.5	91.3	58.2	92.7
	PH_3	16.5	5.7	13.9	0	0	0	0	15.4	0
Complex **2**	Pd	22.2	27.4	30.2	54.8	19.4	18.1	25.4	25.3	10.6
	L–CH_3	59.3	66.4	54.7	45.2	80.6	81.9	74.6	47.8	89.4
	PH_3	18.5	6.2	15.1	0	0	0	0	26.9	0
Complex **3**	Pd	30.9	24.1	31.3	26.7	18.7	18.3	16.8	22.5	11.4
	L–Ph	69.1	75.9	68.7	73.3	81.3	81.7	83.2	56.6	88.6
	PH_3	0	0	0	0	0	0	0	20.9	0

[a] PPh_3 was replaced by PH_3 in the calculation.

contributor and with relatively less contributions from the phosphine and palladium. The remaining three absorptions at 355, 336 and 295 nm are also qualitatively similar to that at 416 nm, with varying degree of contributions from the three fragments.

3.3. Catalysis

3.3.1. C–C cross-coupling reactions

The fact, that palladium complexes are well known to serve as efficient catalysts in bringing about C–C cross-coupling reactions of different types [11], led us to explore such catalytic properties in the present group of complexes. The catalytic activity of these complexes was examined for C–C cross-coupling reactions of three types, *viz.* Suzuki, Heck and Sonogashira reactions.

Initially all the three complexes were tested as catalyst in the Suzuki coupling of phenylboronic acid and *p*-iodoacetophenone to yield the biphenyl product. After extensive optimization, it was found that 0.001 mol% catalyst, 1.7 eqv. Na_2CO_3 as base, ethanol as solvent, 75 °C reaction temperature, and 9 h reaction time, furnished an excellent (>99%) yield of the desired C–C coupled product.[2] Though all the three complexes were found to show comparable catalytic efficiency, the best result was obtained with complex **3** as the catalyst.[2] The scope of the reaction is shown in Table 6, where only the results obtained with complex **3** as the catalyst are presented. Several cross-coupling reactions were performed by varying both the aryl halide and the arylboronic acid. Coupling of phenylboronic acid with three 4-R_1-phenyl iodides (R_1 = CH_3CO, CHO and CN) were tried, all of which afforded the expected C-C coupled products in excellent yields with high ($\sim 10^5$) turnover numbers (entries 1–3). It may be mentioned here that such high turnover numbers are relatively less common [12]. Coupling of *para*-iodoacetophenone with three 4-R_2-phenylboronic acids (R_2 = OCH_3, CH_3 and Cl) also took place with similar efficiency (entries 4–6). A similar trend was observed with the aryl bromides (entries 7–12), however, with a higher catalyst loading (0.01 mol%). The attempted C–C coupling involving aryl chlorides also proceeded smoothly, but with much higher catalyst loading (0.1 mol%) and slightly harsh reaction condition (entries 13–18). It is worth mentioning here that formation of new molecules through C–Cl bond activation is industrially very important due to easy availability of the relatively inexpensive aryl chlorides [13]. Attempts to bring about similar C–C coupling via C–F bond activation of aryl fluoride, however, was unsuccessful (entry 19).

Encouraged by the facile Suzuki coupling reactions catalyzed by complex **3**, we further investigated the catalytic activity of the same complex in Heck reaction of different aryl halides with butyl acrylate. Heck reactions of four *para*-substituted phenyl iodides and butyl acrylate were found to proceed well in 1:1 ethanol-toluene with 0.05 mol% catalyst to afford the coupled products in fairly

[2] Yields of the products obtained with complex **1**, complex **2** and complex **3** as catalyst are 93%, 96% and >99% respectively.

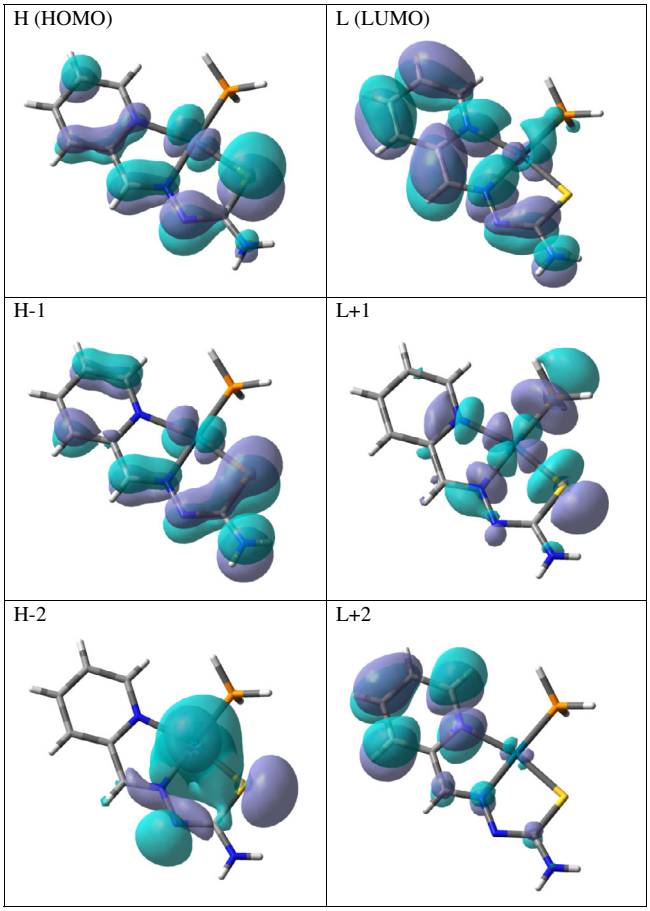

Fig. 3. Contour plots of selected molecular orbitals of complex **1** (PPh_3 was replaced by PH_3 in the calculation).

good yields (entries 1–4, Table 7). For similar reactions with *para*-substituted phenyl bromides catalyst loading needed to be doubled (entries 5–8). However, for *para*-substituted aryl chlorides, much higher catalyst loading (1 mol%), higher temperature and a different solvent medium (polyethylene glycol) were required to obtain fairly good yields (entries 9–12).

Finally we scrutinized the catalytic efficiency of complex **3** in Sonogashira coupling reaction between aryl halides and phenyl acetylene. The yields of Sonogashira coupling reactions were fairly good (Table 8). As before, the coupling involving aryl iodides was most facile (entries 1–4), and the same involving aryl bromides and chlorides was successively more difficult (entries 5–8 and entries 9–12).

3.3.2. C–N coupling reactions

Encouraged by the facile C–C coupling reactions, we were inclined to try our catalyst for C–N coupling reaction as well. We began our study with the coupling of iodobenzene and *para*-substituted anilines, and as anticipated, the C–N coupling reactions also proceeded smoothly with 0.01 mol% catalyst affording the desired products in good yields (entries 1 and 2, Table 9). Similar smooth coupling was also observed for bromobenzene, but with 0.1 mol% catalyst and longer reaction time (entries 3 and 4). When chlorobenzene was used, higher catalyst loading (1.0 mol%), longer reaction time and a different solvent, *viz.* dioxane, were required to achieve reasonably good yield (entries 5 and 6). We also attempted C–N coupling using fluorobenzene, but the targeted reaction could not be brought about (entry 7). Besides primary amines, the scope for arylation of secondary amines was next investigated using the same catalyst. Two secondary amines, *viz.* morpholine and piperidine, were selected for this purpose. The targeted reactions could be achieved with three types of halobenzenes (*viz.* iodobenzene, bromobenzene and chlorobenzene), with gradually increasing difficulty and decreasing yields (Table 10). Such smooth C–N coupling reactions with good yields are of significant contemporary interest [14].

Table 6
Suzuki cross-coupling of aryl halides with phenylboronic acid.[a]

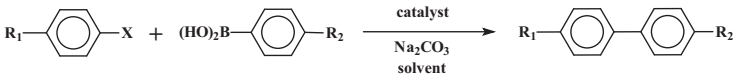

Entry	R_1	R_2	X	Solvent	Temp. (°C)	Time (h)	Amt. of cat. (mol%)	Yield[b] (%)	TON[c]
1	$COCH_3$	H	I	ethanol	75	9	0.001	>99	100000
2	CHO	H	I	ethanol	75	11	0.001	93	93000
3	CN	H	I	ethanol	75	12	0.001	>99	100000
4	$COCH_3$	OCH_3	I	ethanol	75	10	0.001	>99	100000
5	$COCH_3$	CH_3	I	ethanol	75	10	0.001	>99	100000
6	$COCH_3$	Cl	I	ethanol	75	12	0.001	>99	100000
7	$COCH_3$	H	Br	ethanol	75	10	0.01	>99	10000
8	CHO	H	Br	ethanol	75	13	0.01	>99	10000
9	CN	H	Br	ethanol	75	16	0.01	>99	10000
10	$COCH_3$	OCH_3	Br	ethanol	75	13	0.01	>99	10000
11	$COCH_3$	CH_3	Br	ethanol	75	15	0.01	>99	10000
12	$COCH_3$	Cl	Br	ethanol	75	18	0.01	>99	10000
13	$COCH_3$	H	Cl	ethanol:toluene (1:1)	95	12	0.1	88	880
14	CHO	H	Cl	ethanol:toluene (1:1)	95	15	0.1	85	850
15	CN	H	Cl	ethanol:toluene (1:1)	95	20	0.1	81	810
16	$COCH_3$	OCH_3	Cl	ethanol:toluene (1:1)	95	18	0.1	93	930
17	$COCH_3$	CH_3	Cl	ethanol:toluene (1:1)	95	16	0.1	95	950
18	$COCH_3$	Cl	Cl	ethanol:toluene (1:1)	95	18	0.1	92	920
19	$COCH_3$	H	F	polyethylene glycol	110	24	1	0	0

[a] Reaction conditions: aryl halide (1.0 mmol), phenylboronic acid (1.2 mmol), Na_2CO_3 (1.7 mmol), Pd catalyst, solvent (4 mL).
[b] Product detected by GC–MS and yield determined by GC–MS on the basis of residual aryl halide.
[c] TON = turnover number ((mol of product)/(mol of catalyst)).

Table 7
Heck cross-coupling of aryl halides with butyl acrylate.[a]

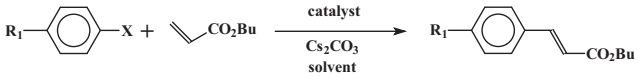

Entry	R_1	X	Solvent	Temp. (°C)	Time (h)	Amt. of cat. (mol%)	Yield[b] (%)	TON[c]
1	H	I	ethanol-toluene (1:1)	110	12	0.05	85	1700
2	$COCH_3$	I	ethanol-toluene (1:1)	110	12	0.05	83	1660
3	CHO	I	ethanol-toluene (1:1)	110	16	0.05	76	1520
4	CN	I	ethanol-toluene (1:1)	110	18	0.05	65	1300
5	H	Br	ethanol-toluene (1:1)	110	14	0.1	72	720
6	$COCH_3$	Br	ethanol-toluene (1:1)	110	14	0.1	74	740
7	CHO	Br	ethanol-toluene (1:1)	110	18	0.1	67	670
8	CN	Br	ethanol-toluene (1:1)	110	20	0.1	59	590
9	H	Cl	polyethylene glycol	150	20	1.0	66	66
10	$COCH_3$	Cl	polyethylene glycol	150	24	1.0	62	62
11	CHO	Cl	polyethylene glycol	150	28	1.0	58	58
12	CN	Cl	polyethylene glycol	150	28	1.0	50	50

[a] Reaction conditions: aryl halide (1.0 mmol), butyl acrylate (1.2 mmol), Cs_2CO_3 (1.7 mmol), Pd catalyst, solvent (4 mL).
[b] Product detected by GC–MS and yield determined by GC–MS on the basis of residual aryl halide.
[c] TON = turnover number ((mol of product)/(mol of catalyst)).

Table 8
Sonogashira cross-coupling of aryl halides with phenylacetylene.[a]

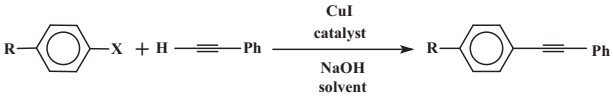

Entry	R_1	X	Solvent	Temp. (°C)	Time (h)	Amt. of cat. (mol%)	Yield[b] (%)	TON[c]
1	H	I	ethanol-toluene (1:1)	110	12	0.01	>99	10000
2	$COCH_3$	I	ethanol-toluene (1:1)	110	12	0.01	>99	10000
3	CHO	I	ethanol-toluene (1:1)	110	14	0.01	>99	10000
4	CN	I	ethanol-toluene (1:1)	110	18	0.01	89	8900
5	H	Br	ethanol-toluene (1:1)	110	16	0.1	>99	1000
6	$COCH_3$	Br	ethanol-toluene (1:1)	110	12	0.1	98	980
7	CHO	Br	ethanol-toluene (1:1)	110	17	0.1	81	810
8	CN	Br	ethanol-toluene (1:1)	110	20	0.1	77	770
9	H	Cl	polyethylene glycol	150	24	1.0	66	66
10	$COCH_3$	Cl	polyethylene glycol	150	24	1.0	>99	100
11	CHO	Cl	polyethylene glycol	150	24	1.0	72	72
12	CN	Cl	polyethylene glycol	150	24	1.0	66	66

[a] Reaction conditions: aryl halide (1.0 mmol), phenylacetylene (1.2 mmol), NaOH (1.7 mmol), Pd catalyst, CuI (10 mol%), solvent (4 mL).
[b] Product detected by GC–MS and yield determined by GC–MS on the basis of residual aryl halide.
[c] TON = turnover number ((mol of product)/(mol of catalyst)).

Table 9
C–N coupling reaction of aryl halides with primary amines.[a]

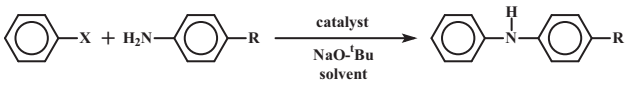

Entry	R	X	Solvent	Temp. (°C)	Time (h)	Amt. of cat. (mol%)	Yield[b] (%)	TON[c]
1	H	I	toluene	95	10	0.01	100	10000
2	OCH_3	I	toluene	95	9	0.01	100	10000
3	H	Br	toluene	95	14	0.1	100	1000
4	OCH_3	Br	toluene	95	15	0.1	100	1000
5	H	Cl	dioxane	110	16	1.0	75	75
6	OCH_3	Cl	dioxane	110	18	1.0	79	79
7	H	F	dioxane	110	24	1.0	0	0

[a] Reaction conditions: aryl halide (1.0 mmol), amines (1.0 mmol), NaO^t-Bu (1.7 mmol), Pd catalyst, toluene (4 mL).
[b] Product detected by GC–MS and yield determined by GC–MS on the basis of residual aryl halide.
[c] TON = turnover number ((mol of product)/(mol of catalyst)).

Table 10
C–N cross-coupling reaction of aryl halides with secondary amines.[a]

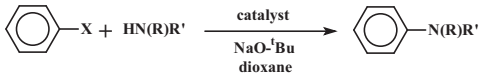

Entry	X	Amine	Temp. (°C)	Time (h)	Amt. of cat. (mol%)	Yield[b] (%)	TON[c]
1	I		110	12	0.01	69	6900
2	I		110	14	0.01	65	6500
3	Br		110	18	0.1	59	590
4	Br		110	18	0.1	62	620
5	Cl		130	24	1	56	56
6	Cl		130	24	1	50	50

[a] Reaction conditions: aryl halide (1.0 mmol), amines (1.0 mmol), NaO^t-Bu (1.7 mmol), Pd catalyst, toluene (4 mL).
[b] Product detected by GC–MS and yield determined by GC–MS on the basis of residual aryl halide.
[c] TON = turnover number ((mol of product)/(mol of catalyst)).

The present study thus demonstrates that complexes **1**–**3** can efficiently catalyze both C–C and C–N coupling reactions. Another noticeable aspect of the observed catalysis is that no additional ligand was necessary, and such ligand-free catalysis is relatively less common [15]. The good catalytic activity of these complexes may be attributed partly to the presence of soft PPh_3 ligand and partly to the presence of S-donor thiosemicarbazone ligand in them, which probably have supported palladium(0), generated *in situ*.

4. Conclusions

The present study shows that thiosemicarbazones of 2-formylpyridine, 2-aceylpyridine and 2-benzoylpyridine can readily interact with the metal center in $[Pd(PPh_3)_2Cl_2]$, and by virtue of having the pyridine-nitrogen as a readily available donor atom, bind to palladium in the NNS-mode without any rotation around the pre-existing imine bond. The resulting complexes **1**–**3** are found to be efficient catalysts for both C–C and C–N coupling reactions.

Acknowledgments

We sincerely thank the reviewers for their constructive comments, which were very useful in preparing the revised manuscript. Financial assistance received from the Department of Science and Technology, West Bengal, India [Grant No. 746(Sanc.)/ST/P/S&T/2G-4/2013] is gratefully acknowledged. Piyali Paul thanks the Council of Scientific and Industrial Research, New Delhi, for her fellowship [Grant No. 09/096(0588)/2009-EMR-I].

Appendix A. Supplementary material

CCDC 958099 and 890279 contains the supplementary crystallographic data for complexes **1** and **3**, respectively. These data can be obtained free of charge from The Cambridge Crystallographic Data Centre via www.ccdc.cam.ac.uk/data_request/cif. Supplementary data associated with this article can be found, in the online version, at http://dx.doi.org/10.1016/j.ica.2014.10.010.

References

[1] (a) J.L. Hickey, P.S. Donnelly, Coord. Chem. Rev. 256 (2012) 2367;
(b) A. Garoufis, S.K. Hadjikakou, N. Hadjiliadis, Coord. Chem. Rev. 253 (2009) 1384;
(c) T.S. Lobana, R. Sharma, G. Bawa, S. Khanna, Coord. Chem. Rev. 253 (2009) 977;
(d) A.G. Quiroga, C.N. Ranninger, Coord. Chem. Rev. 248 (2004) 119;
(e) J.R. Dilworth, P. Arnold, D. Morales, Y.L. Wong, Y. Zheng, Mod. Coord. Chem. (2002) 217;
(f) D.X. West, A.E. Liberta, S.B. Padhye, R.C. Chikate, P.B. Sonawane, A.S. Kumbhar, R.G. Yerande, Coord. Chem. Rev. 123 (1993) 49;
(g) D.X. West, S.B. Padhye, P.B. Sonawane, Struct. Bond. 76 (1992) 1;
(h) S.B. Padhye, G.B. Kaffman, Coord. Chem. Rev. 63 (1985) 127;
(i) M.J.M. Campbell, Coord. Chem. Rev. 15 (1975) 279.
[2] (a) B.K. Dey, P. Paul, S. Bhattacharya, J. Indian Chem. Soc. 91 (2014) 359;
(b) P. Paul, D.K. Seth, M.G. Richmond, S. Bhattacharya, RSC Adv. 4 (2014) 1432;
(c) S. Halder, P. Paul, R. Acharyya, F. Basuli, A. Mukherjee, U. Sanyal, S. Bhattacharya, J. Indian Chem. Soc. 90 (2013) 771;
(d) J. Dutta, S. Bhattacharya, RSC Adv. 3 (2013) 10707;
(e) P. Paul, P. Sengupta, S. Bhattacharya, J. Organomet. Chem. 724 (2013) 281;
(f) S. Datta, D.K. Seth, R.J. Butcher, S. Gangopadhyay, P. Karmakar, S. Bhattacharya, Inorg. Chim. Acta 392 (2012) 118;
(g) J. Dutta, S. Datta, D.K. Seth, S. Bhattacharya, RSC Adv. 2 (2012) 11751;
(h) S. Halder, P. Paul, S.M. Peng, G.H. Lee, A. Mukherjee, S. Dutta, U. Sanyal, S. Bhattacharya, Polyhedron 45 (2012) 177;
(i) P. Paul, S. Datta, S. Halder, R. Acharyya, F. Basuli, R.J. Butcher, S.M. Peng, G.H. Lee, A. Castineiras, M.G.B. Drew, S. Bhattacharya, J. Mol. Cat. A: Chem. 344 (2011) 62.
[3] (a) S.M.S. Hussain, M.B. Ibrahim, A. Fazal, R. Suleiman, M. Fettouhi, B.E. Ali, Polyhedron 70 (2014) 39;
(b) S. Keesara, S. Parvathaneni, G. Dussa, M. Rao, J. Organomet. Chem. 765 (2014) 31;
(c) G.A. Edwards, M.A. Trafford, A.E. Hamilton, A.M. Buxton, M.C. Bardeaux, J.M. Chalker, J. Org. Chem. 79 (2014) 2094;
(d) D. Saha, R. Sen, T. Maity, S. Koner, Langmuir 29 (2013) 3140;
(e) M. Pérez-Lorenzo, J. Phys. Chem. Lett. 3 (2012) 167;
(f) H. Li, C.C.C.J. Seechurn, T.J. Colacot, ACS Catal. 2 (2012) 1147;
(g) H.U. Blaser, B. Pugin, Chim. Oggi. 29 (2011) 62;
(h) V.L. Budarin, P.S. Shuttleworth, J.H. Clark, R. Luque, Curr. Org. Chem. 7 (2010) 614.
[4] (a) S. Nadri, E. Raffice, S. Jamali, M. Joshaghni, Tetrahedron Lett. 55 (2014) 4098;
(b) A.R. Hajipour, F. Dordahan, F. Rafiee, Appl. Organomet. Chem. 27 (2013) 704;
(c) D.S. Surry, S.L. Buchwald, Chem. Sci. 2 (2011) 27;
(d) L. Chen, G.A. Yu, F. Li, X. Zhu, B. Zhang, R. Guo, X. Li, Q. Yang, S. Jin, C. Liu, S.H. Liu, S. Nadri, E. Rafiee, S. Jamali, M. Joshaghani, J. Organomet. Chem. 695 (2010) 1768.
[5] H.L. Grube, 2nd ed., in: G. Brauer (Ed.), Handbook of Preparative Inorganic Chemistry, 2, Academic Press, London, 1965, p. 1584.
[6] S. Chandra, K.K. Sharma, Synth. React. Inorg. Met. –Org. Chem. 12 (1982) 415.

[7] M.J. Frisch, G.W. Trucks, H.B. Schlegel, G.E. Scuseria, M.A. Robb, J.R. Cheeseman, J.A. Montgomery Jr., T. Vreven, K.N. Kudin, J.C. Burant, J.M. Millam, S.S. Iyengar, J. Tomasi, V. Barone, B. Mennucci, M. Cossi, G. Scalmani, N. Rega, G.A. Petersson, H. Nakatsuji, M. Hada, M. Ehara, K. Toyota, R. Fukuda, J. Hasegawa, M. Ishida, T. Nakajima, Y. Honda, O. Kitao, H. Nakai, M. Klene, X. Li, J.E. Knox, H.P. Hratchian, J.B. Cross, V. Bakken, C. Adamo, J. Jaramillo, R. Gomperts, R.E. Stratmann, O. Yazyev, A.J. Austin, R. Cammi, C. Pomelli, J.W. Ochterski, P.Y. Ayala, K. Morokuma, G.A. Voth, P. Salvador, J.J. Dannenberg, V.G. Zakrzewski, S. Dapprich, A.D. Daniels, M.C. Strain, O. Farkas, D.K. Malick, A.D. Rabuck, K. Raghavachari, J.B. Foresman, J.V. Ortiz, Q. Cui, A.G. Baboul, S. Clifford, J. Cioslowski, B.B. Stefanov, G. Liu, A. Liashenko, P. Piskorz, I. Komaromi, R.L. Martin, D.J. Fox, T. Keith, M.A. Al-Laham, C.Y. Peng, A. Nanayakkara, M. Challacombe, P.M.W. Gill, B. Johnson, W. Chen, M.W. Wong, C. Gonzalez, J.A. Pople, Gaussian Inc, Wallingford CT, 2004.
[8] G.M. Sheldrick, SHELXS-97 and SHELXL-97, Fortran programs for crystal structure solution and refinement, University of Gottingen, Gottingen, Germany, 1997.
[9] (a) S. Chandra, S. Raizada, R. Verma, J. Chem. Pharm. Res. 4 (2012) 1612;
(b) S. Budagumpi, R.A. Haque, A.W. Salman, Coord. Chem. Rev. 256 (2012) 1787;
(c) S.A. Elsayed, A.M. El-Hendawy, S.I. Mostafa, I.S. Butler, Inorg. Chim. Acta 363 (2010) 2526;
G.P. Chiusoli, M. Catellani, M. Costa, E. Motti, N. Della, Coord. Chem. Rev. 254 (2010) 456;
(d) S.K. Chattopadhyay, S. Ghosh, Inorg. Chim. Acta 163 (1989) 245.
[10] T.S. Lobana, G. Bawa, A. Castineiras, R.J. Butcher, Chem. Commun. 10 (2007) 506.
[11] (a) L. Meng, C. Liu, W. Zhang, C. Zhou, A. Lei, Chem. Commun. 50 (2014) 1110;
(b) P. Li, B. Lu, C. Fu, S. Ma, Org. Biomol. Chem. 11 (2013) 98;
(c) X. Zhou, J. Luo, J. Liu, S. Peng, G. Deng, Org. Lett. 13 (2011) 432;
(d) S. Teo, Z. Weng, T.S. Andy Hor, J. Organomet. Chem. 696 (2011) 2928;
(e) V. Polshettiwar, C. Len, A. Fihri, Coord. Chem. Rev. 253 (2009) 2599. 253;
(f) C. Barnard, Platinum Met. Rev. 52 (2008) 38;
(g) A. Fihri, P. Meunier, J.C. Hierso, Coord. Chem. Rev. 251 (2007) 2017;
(h) R.B. Bedford, C.S.J. Cazin, D. Holder, Coord. Chem. Rev. 248 (2004) 2283;
(i) C.J. Elsevier, Coord. Chem. Rev. 185 (1999) 809.
[12] (a) G.K. Rao, A. Kumar, S. Kumar, U.B. Dupare, A.K. Singh, Organometallics 32 (2013) 2452;
(b) K. Wang, T. Yi, X. Yu, X. Zheng, H. Fu, H. Chen, R. Li, Appl. Organomet. Chem. 26 (2012) 342;
(c) Q.L. Luo, J.P. Tan, Z.F. Li, W.H. Nan, D.R. Xiao, J. Org. Chem. 77 (2012) 8332;
(d) S. Li, Y. Lin, J. Cao, S. Zhang, J. Org. Chem. 72 (2007) 4067;
(e) T.E. Barder, S.D. Walker, J.R. Martinelli, S.L. Buchwald, J. Am. Chem. Soc. 127 (2005) 4685.
[13] (a) B. Karimi, P.F. Akhavan, Inorg. Chem. 50 (2011) 6063;
(b) G.A. Molander, S.L.J. Trice, S.D. Dreher, J. Am. Chem. Soc. 132 (2010) 17701;
(c) M. Guo, Z. Zhu, H. Huang, Q. Zhang, Catal. Commun. 10 (2009) 865;
(d) A.S. Guram, X. Wang, E.E. Bunel, M.M. Faul, R.D. Larsen, M.J. Martinelli, J. Org. Chem. 72 (2007) 5104;
(e) T. Hatakeyama, M. Nakamura, J. Am. Chem. Soc. 129 (2007) 9844.
[14] (a) J.B. Shaik, V. Ramkumar, B. Varghese, S. Sankararaman, Beilstein J. Org. Chem. 9 (2013) 698;
(b) X. Hao, J. Yuan, G.A. Yu, M.Q. Qiu, N.F. She, Y. Sun, C. Zhao, S.L. Mao, J. Yin, S.H. Liu, J. Organomet. Chem. 99 (2012) 706;
(c) J. Li, L. Liu, Y. Zhou, S. Xu, RSC Adv. 2 (2012) 3207;
(d) B.P. Fors, P. Krattiger, E. Strieter, S.L. Buchwald, Org. Lett. 10 (2008) 3505;
(e) L.J. Heng, W.J. Liu, Org. Lett. 6 (2004) 2809.
[15] (a) X. Rao, C. Liu, Y. Xing, Y. Fu, J. Qiu, Z. Jin, J. Org. Chem. 2 (2013) 514;
(b) Q. Zhou, S. Wei, W. Han, J. Org. Chem. 79 (2014) 1454;
(c) A.N. Marziale, D. Jantke, S.H. Faul, T. Reiner, E. Herdtweck, J. Eppinger, Green Chem. 13 (2011) 169;
(d) C. Liu, Y. Zhang, N. Liu, J. Qiu, Green Chem. 14 (2012) 2999;
(e) C. Liu, Q. Ni, F. Bao, J. Qiu, Green Chem. 13 (2011) 1260;
(f) S.M. Islam, P. Mondal, K. Tuhina, A.S. Roy, S. Mondal, D. Hossain, J. Inorg. Organomet. Polym. Mater. 20 (2010) 264;
(g) M. Guo, Z. Zhu, H. Huang, Q. Zhang, Catal. Commun. 10 (2009) 865;
(h) C. Pan, M. Liu, L. Zhang, H. Wu, J. Ding, J. Cheng, Catal. Commun. 9 (2008) 508.